Desalination and Water Treatment
www.deswater.com

doi: 10.1080/19443994.2014.986534

57 (2016) 3358–3371
February

Taylor & Francis
Taylor & Francis Group

Practical and sustainable household seawater desalination using an improved solar still

Subarna Maiti*, Chitrangi Bhatt, Pankaj Patel, Pushpito K. Ghosh*

Solar Energy Group, Process Design and Engineering Cell, CSIR-Central Salt & Marine Chemicals Research Institute, G.B. Marg Bhavnagar 364002, Gujarat, India, Tel. +91 278 2567760, ext. 6950; Fax: +91 278 2567562; emails: smaiti@csmcri.org (S. Maiti), chitrangibhatt@gmail.com (C. Bhatt), Tel. +91 278 2567760, ext. 6951; Fax: +91 278 2567562; email: papatel@csmcri.org (P. Patel), Tel. +91 9426731115; email: pushpitokghosh@gmail.com (P.K. Ghosh)

Received 12 May 2014; Accepted 7 November 2014

ABSTRACT

Conventional seawater desalination plants have so far not been scaled down to household level, at least not in a practical or affordable manner. Solar still technology can fill this void. Studies were conducted with five step-solar stills (1.01 m^2 top glass area) operated (i) conventionally, (ii) after fitting with North–South reflectors in V-trough alignment to raise the incident solar radiation on the still and (iii) after additionally fitting metallic condensers on the sides. Comparative data generated for (i) and (ii) gave an output (day + night) of 2.95 and 5.95 L, respectively, on a typical sunny day in April 2012, and 2.54 and 5.11 L during a typical day in November 2012. Similarly, comparative data of (ii) and (iii) gave values of 4.72, 4.42 and 5.44 L for (ii); 7.06, 5.31 and 6.27 L for (iii), for experiments conducted during typical days in March, June and December 2012, respectively. Output thus followed the trend (iii) > (ii) > (i). The maximum production of potable water with (iii) was 7.27 L m^{-2} d^{-1} on 22 March 2012 with recovery of 40.4% with respect to concentrated (55,000 ppm) seawater charged. The average output of (iii) over 258 d of operation spread over the year was 5.07 L m^{-2} d^{-1}, and the average efficiency with respect to incident radiation on top glass cover was 32.86%. Such a still, which was not only more productive but also easy to operate, clean and maintain, would be an ideal sustainable solution for individual households in the proximity of the sea if the unit can be made affordable. A scaled-up version of the unit at (ii), having 3.02 m^2 top glass area, and with some modifications in aspect ratio, material of construction and number of steps, gave ca. 3.5 times the output of (ii) with 35,000 ppm seawater feed, indicating the scalability of the still in V-trough design.

Keywords: Household seawater desalination; Solar still; V-trough reflectors; Condenser assembly; Enhanced production & recovery; Easy maintenance

1. Introduction

Scarcity of potable water for drinking and cooking is a challenge confronting people living in coastal areas and small islands. Large desalination plants and smaller community-scale plants have been installed in several of the locations and these have no doubt mitigated hardship to a considerable extent. An unmet need is seawater desalination at a household level.

*Corresponding authors.

Table 1 shows a comparison of water purification technologies at a household level. Many of the treatments are suitable for the removal of pathogens from water. Some methods such as the use of adsorbents can selectively remove specific impurities. Dissolved salts can be removed only through distillation or membrane-based technologies. The former is used mainly in large plants, whereas the latter are employed at household levels only when salinity in feed is low (<2,000 ppm TDS). Thus, for example, reverse osmosis (RO) is practised routinely in homes across many countries but these would be unfit for seawater desalination which requires much higher pressure than the <1 MPa pressure normally employed in the present units. Electrodialysis (ED) could, in principle, desalinate water of any salinity but the capital and operating costs tend to be rather high when the feed water salinity rises. Further, the above techniques are dependent on power, variation of which as a function of salinity is shown in Fig. 1 [1,2]. The plots show that the energy requirement increases considerably with salinity of feed water for desalination techniques other than thermal desalination. More important than the energy requirement is the complexity in scaling down such units for seawater desalination at household levels at an affordable cost.

Solar still is a thermal desalination technique which is standalone, requiring no external energy other than the incident solar radiation. However, the low output from the still has limited its utility and alternative solutions for water purification have captured the market. Our focus has been to view the solar still for niche applications where no other practical solution exists at present. Seawater desalination at a household level, for the benefit of coastal communities residing in the vicinity of the sea, is one such niche application. Other non-conventional uses include the concentration of juices, distillation of urine—particularly cow's urine—for medicinal application, concentration of aqueous extracts of herbs, distilled water for application in batteries, etc. In the latter applications,

Table 1
Household water purification technologies

Parameters	Chemical treatment	Adsorbent	UV[a]	UF[b]	NF[c]	RO[d]	ED[e]	Thermal still	SODIS[f]	Solar still
1. Space requirement	Low	Low	Low	Low	Low	Low	Low	Low	Low	High
2. Investment/10 LPD	Low	Low	Low	Low	Medium	High	High	High	Low	High
3. Ease of operation and maintenance	Medium	High	Low	High	High	High	High	High	Low	High
4. Power requirement	No	No	Yes	No	Yes	Yes	Yes	Yes	No	No
5. 24 × 7 × 365 operation	Yes	Yes	Yes	Yes	Yes	Yes	Yes	Yes	No	No
6. Removes turbidity	Yes	No	No	Yes	Yes	Yes	No	Yes	No	Yes
7. Removes bacterial contamination	Yes	Yes	Yes	Yes	Yes	Yes	No	Yes	?	Yes
8. Removes hardness	No	Yes	No	No	Yes	Yes	Yes	Yes	No	Yes
9. Suitable for										
(i) Feed having mild salinity	No	No	No	No	Yes	Yes	Yes	Yes	No	Yes
(ii) Feed having moderate salinity	No	No	No	No	No	No	Yes	Yes	No	Yes
(iii) Seawater	No	No	No	No	No	No	No	Yes	No	Yes
10. Removes odour	No	Yes	No	No	No	No	No	No	No	No
11. Removes arsenic	Yes	Yes	No	No	Partial	Yes	No	Yes	No	Yes
12. Removes fluoride	Yes	Yes	No	No	Partial	Yes	Partial	Yes	No	Yes
13. Removes iron	Yes	Yes	No	No	Partial	Yes	Partial	Yes	No	Yes
14. Removes nitrate	Yes	Yes	No	No	Partial	Yes	Partial	Yes	No	Yes
15. Removes pesticides	Yes	Yes	No	No	Partial	Yes	Partial	Yes	No	Yes

[a]Ultraviolet.
[b]Ultrafiltration.
[c]Nanofiltration.
[d]Reverse osmosis.
[e]Electrodialysis.
[f]Solar disinfection.

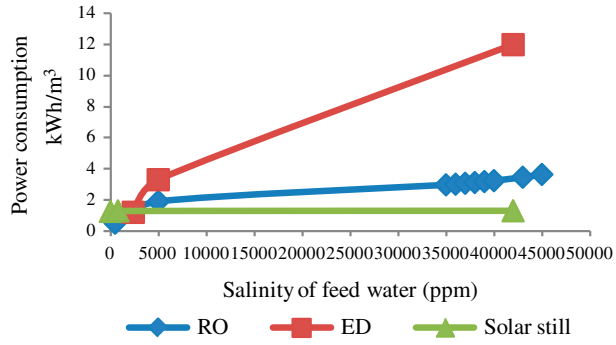

Fig. 1. Variation of power requirement with feed water salinity for electrodialysis, reverse osmosis and solar still.

the lower distillation temperature is an added advantage. There are numerous reports for water distillation using solar still. These describe all possible configurations and include experimental findings, theories and numerical modelling. Comprehensive reviews and cost analysis for various models are also reported in literature. Starting with a basic unit comprising a black-coloured flat basin and a tilted glass cover, several improvisations have been made on the still over the years to raise the output. These include a range of passive and active methods [3–20]. Although not specified explicitly, most of the solar stills can desalinate sea water. However, seawater desalination has its limitation for stills which use wicks, cotton cloth, sponge cubes, charcoal, etc. and also where draining of concentrate is a challenge, leading to scale formation and difficulty in long-term operation.

The present study compares the performances of a single-sloped stepped solar still operated (i) conventionally, (ii) after fitting with North–South reflectors in V-trough alignment to raise the incident solar radiation on the still and (iii) after additionally fitting metallic condensers on the sides. Evaluation was undertaken in the institute's terrace in Bhavnagar (21.77°N, 72.15°E) using normal (35,000 ppm) and concentrated (55,000 ppm) seawater as feed. Additionally, round-the-year data were generated for the still at (iii), while the still at (ii) was scaled up from 1 m^2 to 3 m^2 to ascertain effect of scaling on performance. Improvements from the maintenance point of view are also discussed.

2. Design calculations

2.1. Design of the stepped solar still

Initially, the aim was to produce 5 L of distilled water per day using 1 m^2 of top glass area where the solar radiation was incident. The production from a single-sloped basin-type distillation unit is reported to be about 1–2.5 L of distilled water per m^2 in a day. To enhance the productivity twofold, it was proposed to enhance the solar radiation falling on the feed water and this was done by,

(1) Incorporating reflectors in V-trough alignment along the North–South edges of the still.
(2) Incorporating steps or partitions in the basin.

The steps allowed (i) the water to be held in the tilted position, thus maximizing the absorption of solar beam radiation by the suitably tilted absorber surface, (ii) reduction in the free space thereby maximizing the partial pressure of water vapour, (iii) minimization of the effects due to vapour pressure gradient [21] and (iv) enhancement of the contact area between water and heated basin surface.

Computation of the basin area of stepped solar still fitted with V-trough reflectors for production of a requisite quantity of distilled water is given below. The performance of a solar still is generally expressed as the quantity of water evaporated by unit area of the basin in one day or liters of water obtained per square meter of the basin area per day. The following Eqs. (1–11) [22] help to determine convective and radiative loss coefficients from the still to the atmosphere in terms of top and bottom loss coefficients and finally to calculate the area of the basin which is required to distil the given amount of water. To calculate the basin area and the number of steps the internal heat transfer coefficients were neglected for simplification. The solar radiation absorbed by the water and the basin was assumed to be utilized for evaporation and a fraction for thermal losses. An energy balance for steady state around the water basin can be expressed as: Rate of energy in = Rate of energy out. The relevant equations are summarized below (see symbols provided at the end of the article).

$$I(t)A_S = \dot{Q}_{ew} + \dot{Q}_{losses} \quad (1)$$

$$\dot{Q}_{ew} = (\dot{m}_w)_d L \quad (2)$$

$$\dot{Q}_{losses} = U_L(T_{st} - T_a) \quad (3)$$

wherein $\dot{Q}_{ew}$ is the rate at which thermal energy is utilized for obtaining $(\dot{m}_w)_d$ kg of distilled water per m^2 per day and U_L is the overall heat transfer coefficient from the still to ambient through top and bottom of the unit in Wm^{-2} °C, A_s is the basin area of still in m^2, $I(t)$ is the incident solar radiation in Wm^{-2}. T_{st} is the temperature inside the still and T_a the ambient tem-

perature in ℃. The expression for area of solar still can be given as,

$$A_S = \frac{\dot{Q}_{ew}}{I(t) - \dot{Q}_{losses}} \quad (4)$$

Here

$$U_L = U_t + U_b \quad (5)$$

where U_t and U_b are the top and bottom heat loss coefficients, respectively. Heat is lost from the basin to the ambient through the insulation and subsequently by convection and radiation from the bottom surface of the basin. Hence, the bottom loss coefficient (U_b) can be written as.

$$U_b = K_i/l_i + (h_{cb} + h_{rb}) \quad (6)$$

$$h_{cb} + h_{rb} = 5.7 + 3.8WV \quad (7)$$

U_b is the summation of conduction, convection (h_{cb}) and radiation (h_{rb}) heat transfer coefficients from the bottom to ambient air, WV is the wind velocity in ms^{-1}, K_i and l_i are the thermal conductivity and thickness of the insulation, respectively. The top loss coefficient (U_t) can be written as

$$U_t = h_{rg} + h_{cg} \quad (8)$$

U_t can be determined by considering radiation h_{rg} and convection h_{cg} loss coefficients from the glass cover to the ambient. The radiative heat transfer coefficient between glass and sky is given by

$$h_{rg} = \frac{\epsilon_g \sigma[(T_g + 273)^4 - (T_{sky} + 273)^4]}{T_g - T_a} \quad (9)$$

wherein ϵ_g is the emissivity of glass cover assumed to be 0.88, T_g is the temperature of glass cover and T_{sky} is the effective sky temperature. T_{sky} can be written as

$$T_{sky} = T_a - 6 \quad (10)$$

The convective heat transfer coefficient between glass and sky is given by

$$h_{cg} = 2.8 + 3.0WV \quad (11)$$

Now since A_g is assumed to be 1 m^2, if the total design inner basin liner area (A_s) is computed and found to be >1 m^2 from Eq. (4) for the requisite volume of water per day, steps are needed to be incorporated, such that the outer basin area is fixed in m^2 to accommodate the glass area. Hence, to find the number of steps needed, we have,

$$A_s = 1 + n\,A_{step} \quad (12)$$

where the first term (number 1) on the R.H.S denotes the outer area of the basin liner in m^2, n is the number of steps needed and A_{step} is the area of each step in m^2. The conditions/assumptions for the design are given in Table 2 and the calculated design parameters are tabulated in Table 3.

2.2. Designing the condenser for enhanced output of distilled water

For the conventional stepped solar still with North-South reflectors as above, the glass cover transmits the incoming solar energy to the inside chamber of the still and also acts as a condensing surface for the water vapour evaporated from the water surface. During this process, the latent heat transferred to the glass cover raises the cover temperature and thereby reduces the temperature difference between the evaporating water surface and the condensing glass cover surface [22]. In order to raise the difference, a metallic condenser with cold water flowing on its outer surface is designed to be attached on the sides of the solar still. The flow rate of the condenser's cooling water was fixed and the area of the condenser was calculated in such a way that 50% more output is obtained

Table 2
Conditions/assumptions for design of the solar still

Location	21.77°N, 72.15°E
Ambient air temperature, T_a	25℃
Glass temperature, T_g	60℃
Wind velocity, WV	5 kmph (1.389 m s^{-1})
Average solar isolation on the still inclined at an angle of 20° to horizontal and fitted with N-S reflectors in V-trough, $I(t)$	835 Wm^{-2}
Average solar insolation on horizontal	500 Wm^{-2}
Latent heat of vaporization of water, L	$2{,}309 \times 10^3$ Jkg^{-1}
Area of each step, A_{step}	0.06 m^2

Table 3
Calculated design parameters (Eqs. (1–12))

U_b	3.742 Wm^{-2} K
U_t	14.477 Wm^{-2} K
$\dot{Q}_{losses}$	728.76 Wm^{-2} K
$\dot{Q}_{ew}$	138.31 Js^{-1}
A_s	1.3 m^2
N	5

from the designed stepped solar still and assuming that condensation takes place through purging of vapour from the sides of the still chamber to the condenser chamber. For an assumed $\dot{m}_{wc}$ in kg h^{-1}, which is the vapour that will be condensed in the attached condenser, the mass flow rate of cool water $\dot{m}$ can be expressed as,

$$\dot{m} = (\dot{m}_{wc}L)/\{C_p(T_{ci} - T_{co})\} \quad (13)$$

where C_p is the specific heat of water in J kg^{-1} $^{\circ}C^{-1}$ and $T_{ci} - T_{co}$ is the temperature rise of the inlet and outlet condenser cooling water due to condensation.

Now, assuming the condenser to be a cross-flow type heat exchanger, the area of the condenser can be calculated as:

$$A_c = \frac{\dot{m}_{wc}L}{U_c LMTD} \quad (14)$$

where LMTD (log mean temperature difference) =

$$\frac{(T_{hi} - T_{ho}) - (T_{co} - T_{ci})}{\ln \frac{T_{hi} - T_{ho}}{T_{co} - T_{ci}}} \quad (15)$$

T_{hi} is the inlet steam temperature and T_{ho} is the outlet water temperature from the condenser chamber. The overall condenser heat transfer coefficient, U_c, can be expressed as:

$$U_c = 1/\left[\frac{1}{h_1} + \frac{b}{k} + \frac{1}{h_2}\right] \quad (16)$$

where h_1 is the heat transfer coefficient between the condenser outer surface and the flowing water stream in Wm^{-2} K^{-1}, b is the thickness of the condenser plate in m, k is its thermal conductivity in Wm^{-1} K^{-1} and h_2 is the heat transfer coefficient on the inside surface of the condenser in Wm^{-2} K^{-1}. Assuming the flow outside the condenser surface to be turbulent, and using the Colburn analogy, the local Nusselt number for a wall at constant temperature can be given as:

$$Nu = 0.0292 Pr^{\frac{1}{3}} Re^{0.8} \quad (17)$$

where Nu, Pr and Re are the Nusselt, Prandtl and Reynold's numbers, respectively.

Now,

$$h_1 = \frac{NuK}{D} \quad (18)$$

where K is the thermal conductivity in Wm^{-1} K^{-1}. For the flow of condensate as ripples on the inner wall of the condenser tilted at an angle of $\theta = 20^{\circ}$ from horizontal,

$$1.08R_{el}^{1.22} - 5.2 = \frac{4D(T_{hi} - T_{ho})k_w}{\mu L}\left(\frac{g\cos\theta}{\mu^2}\right)^{1/3} \quad (19)$$

where R_{el} is the film Reynold's number, k_w is the thermal conductivity of condensate at mean film temperature in Wm^{-1} K^{-1}, μ is the dynamic viscosity in $kgm^{-1}s^{-1}$ and D is the vertical length of the condenser plate in m. Using the correction proposed by Kutateladze, 1963, the condensate side heat transfer coefficient can be written as:

$$\frac{h_2}{k_w}\left(\frac{\mu^2}{g\cos\theta\rho^2}\right)^{\frac{1}{3}} = \frac{R_{el}}{1.08R_{el}^{1.22} - 5.2} \text{ for } 30 < R_{el} < 1600 \quad (20)$$

The conditions/assumptions for designing the side condensers of the stepped solar still in Section 2.1 are given in Table 4 and the calculated design parameters for the side condensers are given in Table 5.

3. Fabrication and experiments

3.1. Construction of the prototype solar still

For the solar distillation unit fitted with side condensers, the frame of the solar still was made of teak wood. The basin was made up of single moulded black fibre glass-reinforced plastic (FRP) and had dimensions 1.2 m × 0.85 m × 0.05 m. The dimensions of the steps or partitions were 1.2 m × 0.012 m × 0.05 m. A jacket of 0.006 m plywood was positioned at the sides and the bottom of the still and the annular space was filled with sawdust. Reflectors, made of anodized aluminium sheets (0.0005 m), having the same dimensions as the still, were attached on 0.019 m PVC sheet

Table 4
Conditions/assumptions for designing the side condensers of the stepped solar still

Saturated steam temperature, T_{hi}	80°C
Condensate temperature, T_{ho}	70°C
Cooling water inlet temperature, T_{ci}	30°C
Cooling water outlet temperature, T_{co}	35°C
Condenser load $\dot{m}_{wc}$	0.0625 kg h^{-1}
Vertical length of condenser plate, D	1 m
Angle of the condenser w.r.t horizontal, θ, degrees	20
Density at mean film temperature, ρ	974.8 kgm^{-3}
Thermal conductivity at mean film temperature, k_w	0.672 Wm^{-1} K^{-1}
Dynamic viscosity at mean film temperature, μ	381×10^{-6} kgm^{-1} s^{-1}
Thickness of condenser plate, b	0.0002 m
Thermal conductivity of the material of construction of the condenser plate, k	205 Wm^{-1} K^{-1}

Table 5
Calculated design parameters of the side condensers (Eqs. (14–20))

h_1	28.49 Wm^{-2} K
h_2	7,045.89 Wm^{-2} K
LMTD	7.21°C
U_c	28.38 Wm^{-2} K
A_c	0.196 m^2

and fixed on the North–South edges of the still. The angle of the reflectors could be changed according to the seasonal movement of the sun. The unit was oriented facing south and tilted at 20° to the horizontal. This inclination also helped maximize solar insolation on the glass cover. The cover material was 0.006 m commercial glass which was fixed to a teakwood frame positioned on the still over a rubber gasket strip. The cover could be removed with the use of suitable handles to access the interior for cleaning purposes. Metal-threaded (hole of diameter 0.025 m) Teflon stoppers were attached at the bottom of the still to remove the concentrated saline water. Product water line was made using PVC channel. The condensers on both the sides were made using aluminium sheets of 0.001 m thickness. The size of each condenser was 0.9 m × 0.109 m × 0.05 m. The total area of condensing surface was 0.196 m^2 based on heat transfer calculations. A tray above the condenser had a depth of 0.028 m. A metallic cover with thermocol insulation was placed on the trays. To facilitate steam condensing on the inner top surface of the condenser, water was allowed to flow over the outer surface. The condenser water flowing out was collected in pots during the day time and stored. In the evening the water was transferred to an insulated tank positioned behind the still using d.c. pump, operated by a 20 watt photovoltaic panel. The tank was kept open to atmosphere at night to facilitate night sky radiative cooling. The same water was then used as condenser water the following day.

3.2. Experimental procedure

For the still with condensers, the insulated tank was covered every morning at around 8.00 am and 18 L of sea water of TDS 55,000–60,000 ppm (the seawater salinity was enhanced through evaporation in the institute's salt pan) was poured in the still from a holding tank at around 9.00 am. Higher salinity of feed water was taken to demonstrate the versatility of the solar still. Values of parameters like $I(t)$ on the glass cover, T_g, T_w, T_a and $(m_w)_{ms}$ and $(m_w)_c$ were noted hourly for each day starting from 10.30 to 17.30 h. The T_{cw} at the start of the experiment was recorded. The glass cover and the reflectors were cleaned free of dust/dirt particles each morning before the start of data collection. The night time production, i.e. from 18.30 to 9.30 h the next day was measured the following day. The 24 h production was denoted as $(m_w)_d$. Since the effluent was discharged daily by opening the Teflon stoppers, and fresh seawater charged, scale formation was minimized to a great extent. However, the still was taken for general maintenance once every two months. This included cleaning the basin and inlet and outlet pipes, painting the stands, checking for leaks, cleaning the insulated tank, etc.

3.3. Measurements

Total dissolved solid (TDS) was measured by Eutech CON 700 & Milwaukee SM801 pH/EC/TDS combined meter. All temperatures were measured with RTDs with basic accuracy of ±0.5°C/EU at 30°C. Near

infrared (NIR) solar spectral data were obtained using a spectroradiometer (International Light Technologies ILT 900 W) having a spectral accuracy of ±0.5 nm. $I(t)$ during the operation period was measured using Kipp & Zonen CM4 high temperature pyranometer. The sensitivity of the instrument was 4–10 $\mu V.W^{-1}.m^{-2}$ and response time < 8 s. This pyranometer was suitable for measuring the enhanced radiation falling on the top glass cover of the still due to the reflectors. The wind speed was measured using CFM thermo-anemometer having a measurement range of 0.40–30.00 ms^{-1}. The accuracy for wind speed was ±3%. Ambient air temperature of −10 to 60°C could be measured using the same instrument with an accuracy of ±2.0°C. The measuring cylinder used could measure up to 2,000 mL and had an accuracy of ±5 mL.

4. Results and discussion

As mentioned above, although numerous improvements have been made over the years on the design of solar still, data on incremental improvements starting with a basic solar still are difficult to obtain. Hence, we sought to gather such systematic data for a stepped solar still (Fig. 2). As can be seen from Fig. 2, steps enabled the stagnant feed water in the basin to be held in an inclined position parallel to the incline of the top glass cover.

The specific improvements considered in the study were: (i) effect of reflectors in V-trough configuration and (ii) effect of external condensers. These are discussed in detail below.

4.1. Effect of North-South reflectors in V-trough alignment

In many places where solar stills are intended to be placed, there is a shortage of space, for example in slums. The use of reflectors to increase the solar radiation incident on the still enables vertical utilization of space in these circumstances. It has also been the experience that the basin made of FRP tends to be the costliest part of the still. Hence, minimizing the basin area is of importance for economic considerations also. The reflectors worked according to the principle of a simple non-imaging concentrating collector and exposed the top glass cover to a higher $I(t)$. This was akin to the use of reflectors in low concentration photovoltaic V-trough system [23].

As shown in Fig. 3, spectroradiometer data generated on a sunny day in March showed an average enhancement of ca. 50% in the intensity of the infrared radiation (758.2–949.4 nm) on the glass cover when data were compared for two solar stills with similar configurations—one having reflectors in V-trough and the other without (Fig. 4). Table 6 provides data on the pure water productivity from 55,000 ppm feed on two separate days of the year. It can be seen that the presence of reflectors on the North–South edges of the basin enhanced the productivity of the still by 100%. An experiment was further conducted on the still assembly with reflectors to ascertain leakage of uncondensed vapours. For this purpose, the still was placed on a balance and weight loss was measured at hourly

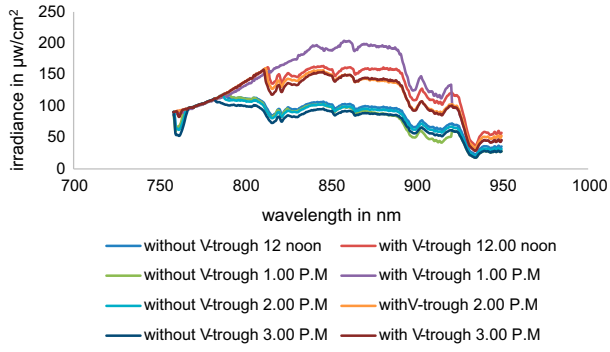

Fig. 3. Spectroradiometer data for the stills: one with V-trough reflector and other without.

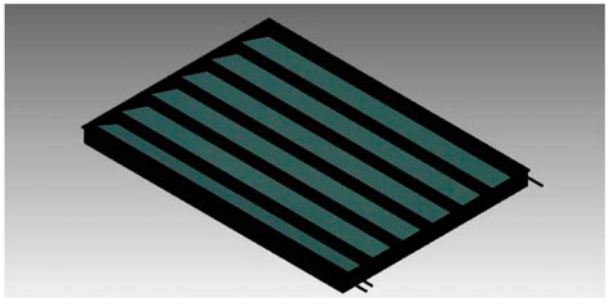

Fig. 2. Still basin in slope showing stagnant water in gray between steps.

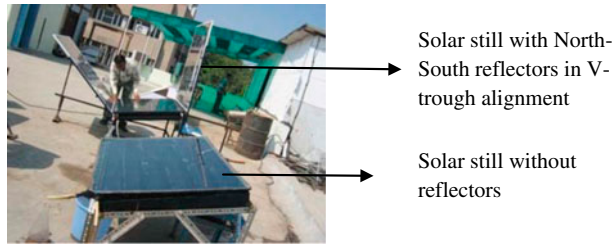

Fig. 4. Experimental set-up atop the institute's terrace, for the comparison of identical stepped solar stills with and without North–South reflectors.

Table 6
The effect of North-South reflectors on still with $1m^2$ tilted basin on two sunny days in the year

Date of expt.	29.04.12		29.11.12	
T_a, °C[a]	36.1		28	
Reflector	Without	With	Without	With
$I(t)$, Wm^{-2}[b]	851.23	1321.04	792.62	1221.19
Product, L	2.95	5.95	2.54	5.11

[a]Average ambient temperature from 10:30 to 17:30 h.
[b]Average solar intensity on glass cover from 10:30 to 17:30 h.

intervals along with the volume of condensate collected. Weight loss was marginally higher than the volume of water collected, but the discrepancy was only of the order of ca. 5%.

4.2. Effect of side condensers

Data were collected for two stills simultaneously, the still with reflectors shown in Fig. 4, and another similar still fitted with side condensers over which naturally cooled water was allowed to flow at 0.2 Lpm (Fig. 5). The two units were placed side by side to compare the relative productivity and the data are summarized in Table 7.

In the absence of condenser, the still output was 5.44 L on 12 December 2012, whereas it was 4.72 L on 14 March and 4.42 L on 21 June. These observations are consistent with the temperature difference between the water and glass surfaces arising from the energy gain from incident solar radiation and release of latent heat from condensing water vapour to the glass surface. The latter, in turn, is dissipated to the surrounding influenced by the combination of ambient temperature and wind speed. Upon incorporation of the side condensers, the ratio of output from condenser and main still were 1.78, 0.85 and 1.10 on 14 March, 21 June and 12 December, respectively. Consequently, even though the output from the main still was lowest (2.48 L) on 14 March, the overall output from the still was 7.06 L compared to 5.31 and 6.27 L on 21 June and 12 December, respectively. The overall output with condensers rose 49.6, 15.3 and 20.1% on these three days. The much higher output on 14 March is attributed to highest insolation on that day—leading to highest rate of evaporation—combined with efficient condensation of the vapour due to the night sky-cooled condenser water.

An important observation on all three days was the considerably lower glass temperature in the still with condensers. This is attributed to the reduced condensation on the glass, leading to less heating up upon release of latent heat. Indeed, the temperature of the glass cover without any water in the still was similar to the temperature of the glass cover when the still was fitted with condenser. Another observation presumably related to the above was that the glass cover in the still with condenser remained much clearer compared to the one without condenser (Fig. 6). No doubt this facilitated greater penetration of the incoming solar rays which, in turn, favoured evaporation. To understand better the interaction among the various measured parameters on a single day, the hourly variations in these parameters during the daytime on 14 March are represented graphically in Fig. 7.

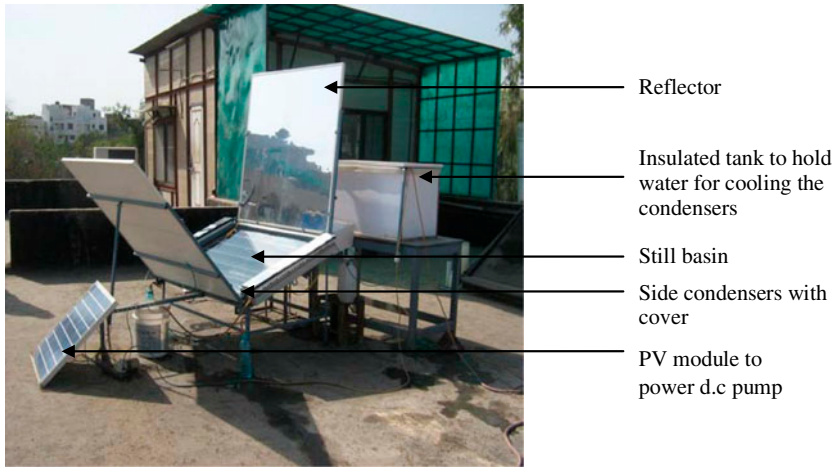

Fig. 5. Photograph of the solar still with reflector and condenser.

Table 7
The effect of side condensers on productivity on three typical days in the year

Date of expt.	14.03.12						21.06.12						12.12.12					
$I(t)$, Wm^{-2}[a]	1,422.39						1,102.15						1,280.64					
T_a, ℃[b]	30.6						39.1						28.8					
WV, ms^{-1}[c]	0.8						1.5						0.55					
Condenser	Without		With				Without		With				Without		With			
T_{cw} ℃	–		20				–		30				–		18			
T_g, ℃[d]	75.5		57.2				72.2		61.6				72.4		60.9			
T_w, ℃[e]	79.5		68.1				74.7		65.3				76.1		66.8			
Product, L		7.06							5.31						6.27			
		4.72	Main still		Condenser		4.42		Main still		Condenser		5.44		Main still		Condenser	
			2.48		4.58				2.86		2.45				2.99		3.29	
	d[f]	n[g]	d	n	d	n	d	n	d	n	d	n	d	n	d	n	d	n
	4.41	0.31	1.99	0.48	4.38	0.2	3.82	0.6	2.43	0.43	2.31	0.14	4.99	0.45	2.58	0.41	3.21	0.08

[a]Average solar intensity on glass cover from 10:30 to 16:30 h.
[b]Average ambient temperature from 10:30 to 17:30 h.
[c]Average wind speed from 10:30 to 17:30 h.
[d]Average glass temperature from 11:30 to 16:30 h.
[e]Average water temperature from 11:30 to 16:30 h.
[f]Day product (L).
[g]Night product (L).

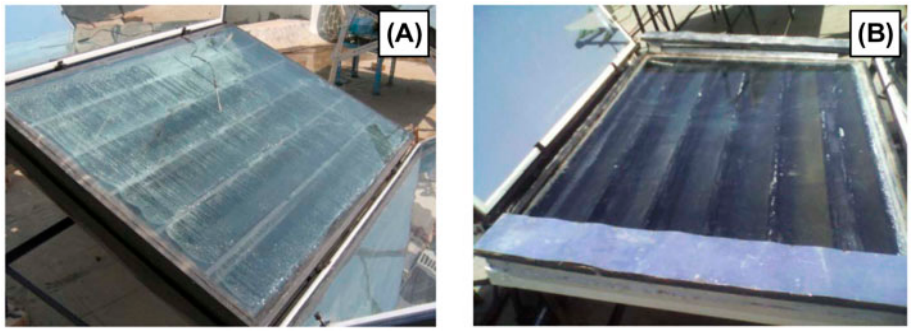

Fig. 6. Photographs showing higher level of haziness of glass cover in the still without condenser (A) and clearer appearance in the still with condenser (B).

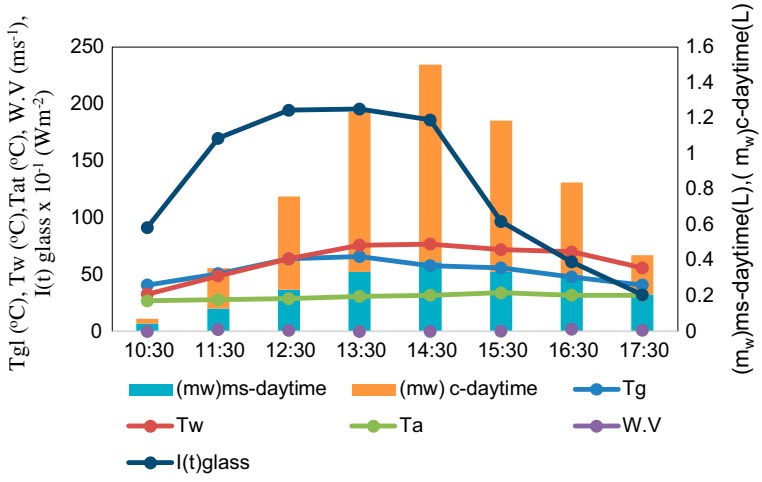

Fig. 7. Hourly plots of $I(t)$, T_a, T_g, T_w $WV.$, $(m_w)_{\text{main still-daytime}}$ and $(m_w)_{\text{condenser-daytime}}$.

4.3. Year round performance data

The still of Fig. 5 was operated for 258 days from February 2012–January 2013 to generate round-the-year data. Fig. 8 provides solar insolation data on a typical day of each month during this period. Output >7 L was obtained on three days in the month of March, the highest being 7.27 L m^{-2} d^{-1} on 22 March, 2012. The recovery based on 55,000 ppm feed water charged was 40.4%. Month-wise average output from the main still and condenser are shown separately in Fig. 9(top). The ratio of output from condenser and main still was in the range of 1.16–1.65 during February to May. During the months of June and October–January, the ratio reduced below 1 (0.77–0.89) and the ratio was least during July–September (0.47–0.50). Fig. 9(bottom) provides data on the ambient conditions and temperature of condenser water. As mentioned above, the latter was allowed to cool through night sky radiation and thereafter, kept in a covered insulated tank during the day time. The key performance indicators of the present still were (i) the ratio of output from the condenser and main still and (ii) the absolute output. Accordingly, the Still Performance Indicator (SPI) was defined as:

$$\text{SPI} = [(m_w)_c/(m_w)_{ms}] \times (m_w)_d \tag{21}$$

The SPI was correlated with $I(t)$, T_a WV and T_{ci} as shown in Eq. (22).

$$\text{SPI} = -9.74 + 7.47I(t) + 0.59T_a - 1.24WV - 0.38T_{ci};\quad R^2 = 0.94 \tag{22}$$

It can be seen from Eq. (22) that for the stepped solar still fitted with reflectors in V-trough alignment and side

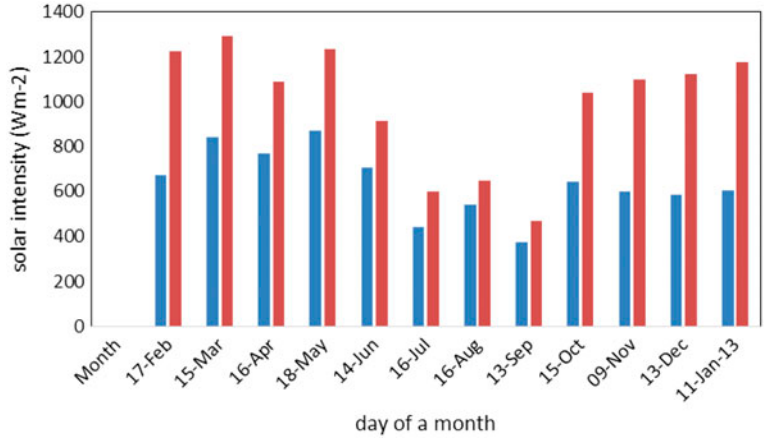

Fig. 8. Global solar insolation (average of 7 h from 10.30 to 17.30 h) on a typical day in each month of the year (blue) and concentrated radiation due to V-trough incident on top glass cover (red).

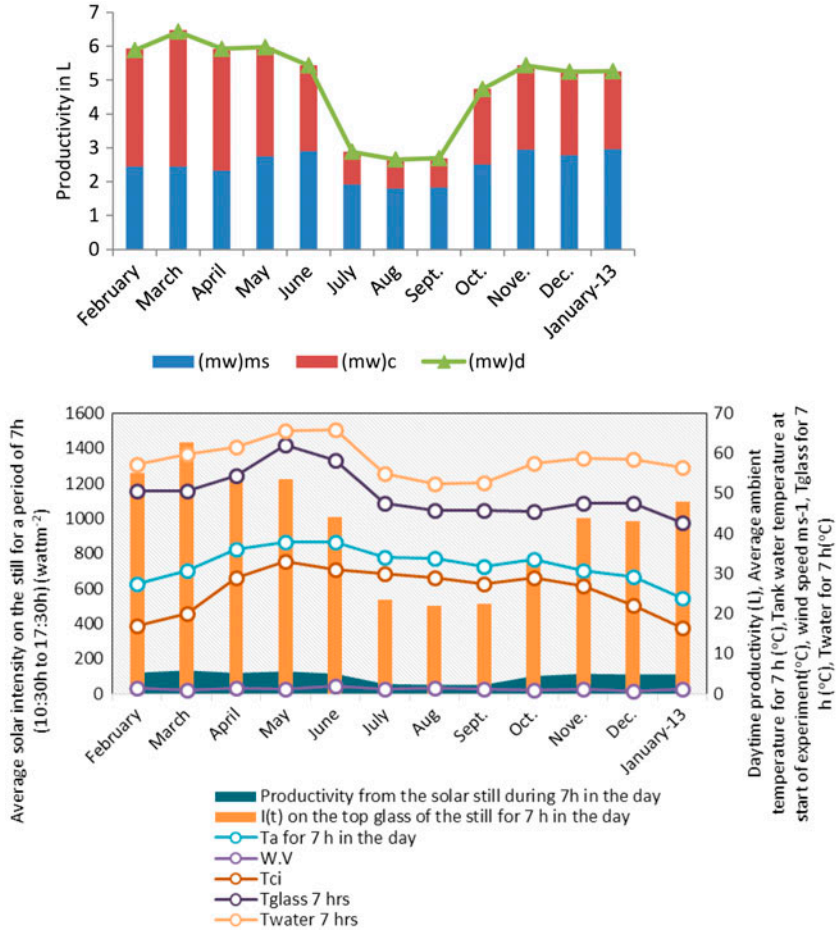

Fig. 9. (Top) Year-round-data for the solar still showing the production of distilled water from the condensers and the still separately. (Bottom) Plot of average monthly ambient temperature conditions ($I(t)$, T_a, $W{\cdot}V$.) and T_{ci} during the experimental period.

condensers, $I(t)$ had a dominant effect. This would also be evident from a comparison of Fig. 9(top) and (bottom), wherein, the water output mirrored $I(t)$ throughout the year. T_a too assisted in the evaporation process, whereas lower T_{ci} favored condensation as indicated by the negative sign. Lower T_{ci} is also indicative of night temperature and wind velocity conditions conducive for cooling, which assisted in night production. Higher WV facilitated condensation on the glass cover of the main still due to enhanced convective loss and accordingly, $(m_w)_c/(m_w)/_{ms}$ decreased. Thus the defined SPI and Eq. (22) nicely accounted for the year-round-data. Whereas Fig. 7 brought out interactions among the measured parameters on a given day, Fig. 9(bottom) shows such interactions averaged over the entire year.

The overall efficiency of the solar still considering total water output over 258 d of operation and total solar energy incident on the still during this period may be expressed as,

$$\eta = \frac{L\sum_1^{258}(m_w)_d}{\sum_1^{258}(E_s)_d} \quad (23)$$

$L \times (m_w)_d$ (J) is the output energy from the still on a given day, wherein, L is the latent heat of vaporisation in $kJkg^{-1}$, and $(E_s)_d$ is the total solar energy (J) incident on the still fitted with reflectors on a given day. The efficiency was computed to be 32.86%.

4.4. Studies on scalability of still fitted with V-trough reflectors

A preliminary study was undertaken to ascertain the scalability of stepped solar still fitted with North–South reflectors in V-trough alignment. For this purpose, production from a 3 m^2 still was assessed against that from the 1 m^2 still with reflectors in Fig. 4, under comparable ambient conditions. The productivity data and weather conditions are provided in Table 8A. It can be seen that the average production from the larger still was nearly 3.5 times that of the 1 m^2 still. The superior results with the larger still may be on account of certain modifications taking cost and performance into account. These are tabulated in Table 8B. Most importantly, the scaled-up still (i) was fabricated from black-powder coated SS316 stainless steel instead of FRP to reduce cost and thickness of the partition walls in the basin, (ii) had a higher aspect ratio to reduce reflective losses from the V-trough reflectors and (iii) could accommodate eight steps instead of the five steps in the 1 m^2 still. The 16–17 L

Table 8A
Comparative data of distilled water production from 1 m^2 and 3 m^2 solar stills fitted with North–South V-trough reflectors along with ambient parameters.

	Date	TDS of feed/ ppm	Average solar intensity on horizontal surface/Wm^{-2}	Average solar intensity on glass cover/Wm^{-2}	$T_{ambient}$ /(℃)	Wind speed/ ms^{-1}	Product water/L
1 m^2 FRP still without condensers	19.03.2012	55,000	848.11	1490.01	33.1	0.8	4.8
	20.03.2013	35,000	776.88	1396.5	33.3	1.2	4.4
3 m^2 SS still without condensers	19.03.2014	35,000	844.08	1467.74	34	1.1	16.99
	20.03.2014	35,000	819.89	1360.21	33.8	0.9	16.32

Table 8B
Similarities and differences in the designs of the 1 m^2 and 3 m^2 solar stills for which production data are shown in Table 8A.

Still Dimensions	4′ × 3′	8′ × 4′
Top glass area	1.01 m^2	3.02 m^2
Basin surface	Black moulded FRP	Powder coating on SS surface
Insulation	Sawdust placed in plywood jacket	Polycarbonate sheet
Step thickness	1.75 cm	0.15 cm
No. of steps	5	8
$A_s = 1 + n\ A_{step}$ (Eq. 12)	1.32 m^2	3.97 m^2
Initial water volume in basin	18 L	60 L
N–S reflectors	Yes	Yes
Condenser	None	None

output achieved with the 3 m^2 still in the most productive month (March) of the year is likely to increase further with the attachment of side condensers.

5. Conclusion

The present study demonstrated that fitting of a 1.01 m^2 stepped solar still with North–South reflectors in V-trough assembly led to ca. twofold increase in distilled water production from concentrated (55,000 ppm) seawater in comparative studies conducted during April and November in Bhavnagar, India. Threefold scale-up of such a design, albeit with some modifications in aspect ratio, material of construction and number of steps, enhanced the production proportionately, confirming the scalability of the design. Experiments were additionally conducted on the smaller still with incorporation of side metallic condensers, which raised the production volume and product water recovery from an average of 4.86 L and 27% to an average of 6.21 L and 35%, respectively, over the three days when comparative studies were undertaken. Round-the-year data collected on this still gave an average output of 5.07 L m^{-2} d^{-1}, while the average efficiency with respect to incident radiation on top glass cover was 32.86%. A regression analysis was also undertaken. The still design additionally facilitated maintenance by introducing a detachable glass cover and openings at the bottom. Considering the difficulties encountered in household desalination of seawater, the present study demonstrated that use of a solar still with enhanced productivity, scalability and ease of maintenance may be an attractive option in coastal locations blessed with ample sunshine, not just in summer months but round the year.

Acknowledgments

CSIR is acknowledged for infrastructure support and the authors thank Mr J.N. Bharadia for assistance in fabrication of the prototype. Project No. CSC 0203 is hereby acknowledged. The PRIS registration number of this manuscript is PRIS/069/2013.

Symbols

A — Top glass area where solar radiation is incident/outer basin area (m^2)
A_c — Area of the condenser (m^2)
A_s — inner basin area of still (m^2)
A_{step} — area of each step (m^2)
b — thickness of condenser plate (cm)
C_p — specific heat of water (J kg^{-1} $°C^{-1}$)
D — vertical length of condenser Plate (m)
$(E_s)_d$ — total solar energy incident on the still (J)
h_1 — heat transfer coefficient between condenser outer surface and flowing water stream (W m^{-2} K)
h_2 — heat transfer coefficient on the inside surface of the condenser (W m^{-2} K)
h_{cb} — convection heat transfer coefficient from bottom to ambient (W m^{-2} K)
h_{cg} — convection loss coefficients from glass cover to ambient (W m^{-2} K)
h_{rb} — radiation heat transfer coefficient from bottom to ambient (W m^{-2} K)
h_{rg} — radiation loss coefficients from glass cover to ambient (W m^{-2} K)
$I(t)$ — incident solar radiation (W m^{-2})
k — thermal conductivity of material of construction of condenser plate (W m^{-1} K^{-1})
k_w — thermal conductivity of condenser plate at mean film temperature (W m^{-2} K)
L — latent heat of vaporization (kJ kg^{-1})
$LMTD$ — logarithmic mean temperature difference
$\dot{m}$ — mass flow rate of cool water
$(\dot{m})_{wc}$ — condenser load (kg h^{-1})
$(m_w)_d$ — mass of distilled water obtained per m^2 per day
$(m_w)_{ms}$ — mass of water obtained from the main still (kg h^{-1})
n — number of steps constructed in the still
Nu — Nusselt number
Pr — Prandtl number
$\dot{Q}_{losses}$ — rate at which thermal energy is utilized for obtaining $(\dot{m}_w)_d$ kg of water per m^2 per day (J s^{-1})
Q_{losses} — amount of heat energy lost during heat transfer (W m^{-2} K)
R_e — Reynold's number
T_a — Ambient temperature (°C)
T_{ci} — Cooling water inlet temperature (°C)
T_{co} — Cooling water outlet temperature (°C)
T_g — Temperature of the glass cover (°C)
T_{hi} — Saturated steam temperature (°C)
T_{ho} — Condensate temperature (°C)
T_{sky} — Effective sky temperature (°C)
T_{st} — Temperature of the inside of the still (°C)
U_b — Bottom heat loss coefficient (W m^{-2} K)
U_c — Condenser overall heat transfer coefficient (W m^{-2} K)
U_L — Overall heat transfer coefficient from still to ambient through top and bottom (W m^{-2}°C)
U_t — Top heat loss coefficient (W m^{-2} K)
WV — Wind velocity (m s^{-1})

Greek

ρ — Density at mean film temperature (kg m^{-3})
μ — Dynamic viscosity (kg $m^{-1}s^{-1}$)
θ — Angle of inclination of condenser from the horizontal
ϵ_g — Emissivity of glass

References

[1] P. Xu, T. Cath, G. Wang, J.E. Drewes, S. Dolnicar, Critical Assessment of Implementing Desalination Technology, Water Research Foundation, Denver, CO, 2010.

[2] E. Korngold, Electrodialysis unit: Optimization and calculation of energy requirement, Desalination 40 (1982) 171–179.

[3] H. Ben Bachaa, K. Zhanib, Contributing to the improvement of the production of solar still, Desalin. Water Treat. 51 (2013) 1310–1318.

[4] A.K. Tiwari, G.N. Tiwari, Effect of water depths on heat and mass transfer in a passive solar still: In summer climatic condition, Desalination 195 (2006) 78–94.

[5] R. Tripathi, G.N. Tiwari, Thermal modeling of passive and active solar stills for different depths of water by using the concept of solar fraction, Sol. Energ. 80 (2006) 956–967.

[6] K. Arshad, B. Janarthanan, S. Shanmugan, Performance of honeycomb double exposure solar still, Desalin. Water Treat. 26 (2011) 260–265.

[7] H.E.S. Fath, H.M. Hosny, Thermal performance of a single-sloped basin still with an inherent built-in additional condenser, Desalination 142 (2002) 19–27.

[8] A.K. Tiwari, G.N. Tiwari, Thermal modeling based on solar fraction and experimental study of the annual and seasonal performance of a single slope passive solar still: The effect of water depths, Desalination 207 (2007) 184–204.

[9] A.K. Rajvanshi, Effect of various dyes on solar distillation, Sol. Energ. 27 (1981) 51–65.

[10] H. Tanaka, Y. Nakatake, Increase in distillate productivity by inclining the flat plate external reflector of a tilted-wick solar still in winter, Sol. Energ. 83 (2009) 785–789.

[11] H.Ş. Aybar, H. Assefi, Simulation of a solar still to investigate water depth and glass angle, Desalin.Water Treat. 7 (2009) 35–40.

[12] V. Velmurugan, C.K. Deenadayalan, H. Vinod, K. Srithar, Desalination of effluent using fin type solar still, Energy 33 (2008) 1719–1727.

[13] B.A.K. Abu-Hijleh, Enhanced solar still performance using water film cooling of the glass cover, Desalination 107 (1996) 235–244.

[14] S.N. Rai, G.N. Tiwari, Single basin solar still coupled with flat plate collector, Energy. Convers. Manage. 23 (3) (1983) 145–149.

[15] A.A. El-Sebaii, M. Al-Dossari, A mathematical model of single basin solar still with an external reflector, Desalin. Water Treat. 26 (2011) 250–259.

[16] Y.P. Yadav, Analytical performance of a solar still integrated with a flat plate solar collector: Thermosiphon mode, Energy. Convers. Manage. 31 (1991) 255–263.

[17] P. Monowe, M. Masale, N. Nijegorodov, V. Vasilenko, A portable single-basin solar still with an external reflecting booster and an outside condenser, Desalination 280 (2011) 332–338.

[18] H. Tanaka, Y. Nakatake, Theoretical analysis of a basin type solar still with internal and external reflectors, Desalination 197 (2006) 205–216.

[19] S. Abdallah, O.O. Badran, Sun tracking system for productivity enhancement of solar still, Desalination 220 (2008) 669–676.

[20] S. Satcunanathan, H.P. Hanses, An investigation of some of the parameters involved in solar distillation, Sol. Energ. 14 (1973) 353–363.

[21] J. Machin, The study of evaporation from small surfaces by the direct measurement of water vapour pressure gradients, J. Exp. Biol. 53 (1970) 753–762

[22] G.N. Tiwari, Solar Energy Fundamentals, Design, Modeling, and Applications, CRC Press, New York, NY, 2002.

[23] S. Maiti, P.K. Ghosh, Indian Patent Application No. 1550/DEL/2009 dated 27th July.